

## Relationships between Land Surface and Near-Surface Atmospheric Variables in the NCEP North American Regional Reanalysis

YAN LUO AND ERNESTO H. BERBERY

*Department of Atmospheric and Oceanic Science/ESSIC, University of Maryland, College Park, College Park, Maryland*

KENNETH E. MITCHELL

*Environmental Modeling Center, National Centers for Environmental Prediction/NOAA, Camp Springs, Maryland*

ALAN K. BETTS

*Atmospheric Research, Pittsford, Vermont*

(Manuscript received 23 October 2006, in final form 24 May 2007)

### ABSTRACT

This study examines the recently released National Centers for Environmental Prediction (NCEP) North American Regional Reanalysis (NARR) products over diverse climate regimes to determine the regional relationships between soil moisture and near-surface atmospheric variables. NARR assimilates observed precipitation, as well as near-surface observations of humidity and wind, while seeking a balance of the surface water and energy budgets with a modern land surface model. The results of this study indicate that for most basins (of approximate size of  $0.5\text{--}1.0 \times 10^6 \text{ km}^2$ ) the NARR surface water budgets have relatively small residuals (about  $0.2 \text{ mm day}^{-1}$ ), and slightly larger residuals (about  $0.4 \text{ mm day}^{-1}$ ) for basins with complex terrain like those in the western United States.

Given that the NARR is an assimilation system (especially one that assimilates observed precipitation), the NARR does not include feedbacks between soil moisture and precipitation. Nonetheless, as a diagnostic tool anchored to observations, the NARR does show that the extent of positive correlation between anomalies of soil moisture and anomalies of precipitation in a given region depends on that region's dryness. The existence of correlations among all variables is a necessary—but not sufficient—condition for land-atmosphere feedbacks to exist, as a region with no correlations would not be expected to have feedbacks. Likewise, a high degree of persistence of soil moisture anomalies in a given basin does not by itself guarantee a positive correlation between anomalies of soil moisture and precipitation.

Land surface-atmosphere relationships at monthly time scales are identified by examining the associations between soil moisture and surface and boundary layer variables. Low soil moisture is consistently associated with increased net shortwave radiation and increased outgoing longwave radiation through the effects of less cloud cover and lower atmospheric humidity. No systematic association is revealed between soil moisture and total net surface radiation, as this relation varies substantially between different basins. Low soil moisture is positively correlated with increased sensible heat and lower latent heat (reflected in a smaller evaporative fraction), decreased low-cloud cover, and higher lifting condensation level. The relation between soil moisture anomalies and precipitation anomalies is found to be quite variable between the basins, depending on whether availability of surface water exceeds the available energy for evaporation, or vice versa. Wetter basins, like the Columbia and Ohio, display weak or no correlations between soil moisture anomalies and precipitation anomalies. On the other hand, transitional regions between wet and dry regions, like the central Great Plains, manifest a positive correlation between soil moisture anomalies and precipitation anomalies. These results further the understanding of previous predictability studies (in coupled land-atmosphere prediction models), which indicates that in order for precipitation anomalies to emerge in response to soil moisture anomalies in a given region, it is necessary that the region's seasonal climate be neither too dry nor too wet.

---

*Corresponding author address:* Ernesto Hugo Berbery, Department of Atmospheric and Oceanic Science/ESSIC, 3427 Computer and Space Sciences Building, University of Maryland, College Park, College Park, MD 20742-2425.  
E-mail: berbery@atmos.umd.edu

## 1. Introduction

The coupling of the atmosphere with slowly evolving sea surface temperatures has the potential to improve the skill of prediction on the long-term seasonal time scales (e.g., Shukla et al. 2000). Since the work of Namias (1958), the importance of the interactions and feedbacks between land surface and precipitation processes has gained increasing interest as well. Land surface–atmosphere interactions relate the underlying soil moisture anomalies with the behavior of the boundary layer and precipitation processes. As soil moisture has a longer memory than typical precipitation events, the lower boundary conditions can feed back into future precipitation events, thus providing useful information to improve the predictive skill in a given region. Studies like those of Betts et al. (1996, 1998) and Betts and Ball (1998) have led to a better understanding of the land surface–boundary layer processes and to the improvement of model parameterizations, while others (e.g., Koster et al. 2000; Schlosser and Milly 2002; Koster and Suarez 2003) have examined the contributions of soil moisture memory processes to seasonal-to-interannual variability and predictions. However, for many regions the knowledge of the contribution of soil moisture memory to the predictive skill remains limited, despite some promising studies (e.g., Koster et al. 2004). Hence it is important to perform by observational and diagnostic means such as in the study here, companion studies of the extent of correlation between soil moisture anomalies and precipitation anomalies in analysis/assimilation systems, especially assimilation systems like the North American Regional Reanalysis (NARR), which assimilate analyses of precipitation.

Soil states strongly influence the surface water and energy budgets, which in turn affect the boundary layer conditions that control weather and climate at different time scales (Betts et al. 1996). Soil moisture reflects past precipitation and evaporation, snowmelt, infiltration, and runoff. In turn, the soil moisture acts as a strong control on the partitioning between sensible heat flux and latent heat flux at the surface (the Bowen ratio) modulating precipitation over a given basin (Eltahir 1998). Wet conditions can lead to larger equivalent potential temperatures, and greater cloudiness and precipitation potential (Entekhabi 1995). Variations in surface soil moisture can thus induce variations in evaporation and sensible heat flux that in turn can affect the evolution of the atmospheric boundary layer. If positive land surface–atmosphere feedbacks exist, then land surface memory due to soil moisture storage could result in enhancing and prolonging both floods and droughts (Entekhabi et al. 1992). Although the focus of

this article is on monthly and longer time scales, it has been shown that for short time scales (diurnal to synoptic) and certain regions, negative feedbacks between soil moisture and precipitation may exist (see, e.g., Findell and Eltahir 2003).

In very wet regions, evapotranspiration tends to remain fairly close to the potential evaporation and thus it is usually insensitive to changes in soil moisture. In extremely dry conditions, evaporation rapidly removes a positive soil moisture anomaly without a significant impact on the atmosphere. In both cases the chances of having enhanced predictive skill from the soil moisture conditions is believed to be slim. A growing number of studies indicate that the larger contributions to monthly-to-seasonal predictive skill of precipitation from soil moisture anomalies come in transition regions between dry and wet zones where evaporation anomalies are large enough and persistent enough (in response to soil moisture anomalies) to modify the precipitation response (Koster et al. 2000, 2002, 2004). In such situations, it can be expected that the slowly varying soil moisture anomalies will persist over enough time to affect the overlying boundary layer, as well as to affect the temporally averaged surface pressure gradient and low-level moisture convergence through persistent changes in surface heating, and thus they can add predictive skill to the forecasts in the given region.

Examples of soil moisture memory and land–atmosphere interactions contributing to the persistence of weather anomalies are not infrequent, and probably among the most discussed are the 1988 summer drought and 1993 floods over the United States. These events have prompted studies that indicate that, in addition to the remote and large-scale effects, regional feedbacks were at play (see, e.g., Beljaars et al. 1996; Trenberth and Guillemot 1996; Bosilovich and Sun 1999; Paegle et al. 1996). Likewise, in the case of the 1998 Oklahoma–Texas drought, Hong and Kalnay (2000, 2002) found that the dry spell was not originated by soil moisture anomalies, but once it was established, the dry anomalies helped maintain the pattern for several months through a positive feedback before the mechanism was overwhelmed by synoptic-scale disturbances in the autumn. Although their results referred to that specific case, their hypotheses are relevant for other cases as well. Studies investigating the influences of soil moisture anomalies on the North American monsoon have found a similar positive feedback (Small 2001).

For a diverse set of basins of North America, particularly those relevant for the Global Energy and Water Cycle Experiment (GEWEX) Americas Prediction Project (GAPP), this article diagnostically examines the relationships and correspondence between soil

moisture and near-surface atmospheric variables and precipitation as represented in NARR. A hallmark feature of the NARR system is its assimilation of hourly precipitation analyses. Consequently, the diagnosis of land–atmosphere relationships based on NARR cannot provide direct measures of feedback between soil moisture and precipitation, since NARR precipitation does not evolve freely in response to model physics. Nevertheless, a diagnostic assessment of NARR can reveal those regions where the correlation between soil moisture and precipitation is strong, and thereby help identify those regions where feedbacks are more likely in nature. On the other hand, a significant feedback between precipitation and soil moisture within a region is very unlikely if a high correlation between them is absent. It is not suggested that a high correlation between soil moisture and precipitation is sufficient by itself to establish the existence of a feedback between them. External forcings such as moisture convergence from outside the region or large-scale dynamics can cause the precipitation anomaly within the region and that in turn cause the corresponding soil moisture anomaly, thus representing a one-way process lacking feedback. We view a high correlation of soil moisture and precipitation within a region as a necessary but not sufficient condition for a feedback between them to be present.

The present paper is organized as follows: section 2 presents the regions of interest, the dataset and its performance in water and energy budgets studies. Section 3 addresses (a) the association between soil moisture and precipitation across various basins, (b) the dependence of this association on the degree of persistence of soil moisture anomalies, and (c) the implications of (a) and (b) on the land surface–atmosphere interactions and the predictive skill of precipitation. Finally, section 4 presents the conclusions.

## 2. Water and energy budgets

### a. The North American Regional Reanalysis

This study employs the NARR dataset developed at the Environmental Modeling Center (EMC) of the National Centers for Environmental Prediction (NCEP). It is expected that this dataset will be most useful not only for energy and water budget studies, but also for the analysis of atmosphere–land relationships like the one presented in this study. NARR is a long-term set of consistent regional analyses developed with the 2003 version of the Eta Model and its associated Eta Data Assimilation System (Mesinger et al. 2006). The domain is about the same as the NCEP's operational regional model, and is depicted in Fig. 1a. The computational grid has a horizontal spacing of 32 km and 45 vertical

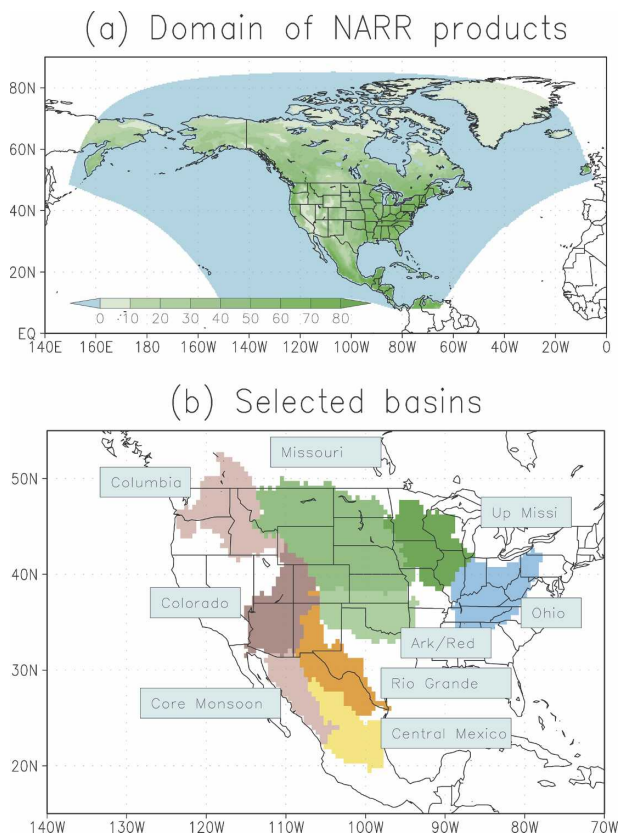


FIG. 1. (a) North American Regional Reanalysis products domain. The fraction (percent) of green vegetation cover for summer (JJAS) is depicted over land. (b) Location of the selected North American basins.

levels. The Eta Model is coupled to a land surface model (LSM) called Noah. It originated in the 1980s with the Oregon State University LSM (Mahrt and Pan 1984; Mahrt and Ek 1984; Pan and Mahrt 1987). Subsequently, many physical improvements were added by researchers at EMC and collaborators (Chen et al. 1996, 1997; Koren et al. 1999; Ek et al. 2003). The Noah LSM simulates land surface temperature, the components of the surface energy balance and the surface water balance, and the evolution of soil temperature and soil moisture, both liquid and frozen, in four soil layers (10, 30, 60, 100 cm thick). The surface infiltration scheme follows Schaake et al. (1996) and accounts for subgrid spatial variability in soil moisture, precipitation, and runoff. The surface evaporation treatment includes direct evaporation from soil, transpiration from vegetation (using the Jarvis–Stewart canopy conductance approach), evaporation of intercepted precipitation, and snow sublimation. The surface layer parameterization in the Noah LSM and NARR is described in Chen et al. (1997). Further development and references for the Noah LSM are given by Ek et al. (2003).

As described by Mesinger et al. (2006), NARR uses many observed quantities in its data assimilation scheme, including gridded analyses of rain gauge precipitation over the continental United States (CONUS), Mexico, and Canada, which is by far the most important data addition over the previous global reanalyses at NCEP. Over CONUS (but not Mexico or Canada) the observed precipitation was adjusted for topographic effects with the Parameter-elevation Regressions on Independent Slopes Model [PRISM; see Daly et al. (1994) for an explanation of this method; Luo et al. (2005) discuss its implications for surface water budgets]. The Climate Prediction Center (CPC) Merged Analysis of Precipitation (CMAP; Xie and Arkin 1997), disaggregated from pentad data to hourly data, is employed over Central America south of Mexico and over oceans south of 42.5°N. Other satellite remote sensing products as well as information from wind profilers and an external daily snow cover analysis are also assimilated in NARR (for details see Mesinger et al. 2006).

Although the precipitation input to the land surface is realistic and the snowpack is updated daily from an external analysis of snow depth, all other NARR variables examined here are basically a function of the model parameterizations: these include soil moisture, runoff, actual and potential surface evaporation, surface sensible and latent heat flux, surface net shortwave and longwave radiation, lifting condensation level (LCL), and cloud cover. It is noted that the representation of the surface water and energy budgets and the corresponding parameterizations vary considerably among models. As shown in a comparison of uncoupled land data assimilation systems forced with identical land surface forcing and using the same specifications of vegetation class and soil class (see Mitchell et al. 2004, and references therein) the resulting surface fields may be significantly different. Consequently, NARR still carries important, but unavoidable, model dependence. Full details on the NARR products can be found online at <http://www.emc.ncep.noaa.gov/mmb/rrean/>. The long-term NARR dataset, which includes 3-hourly temporal resolution, avoids the discontinuities associated with the periodic changes to operational forecast and data assimilation systems. The study here applies the 24-yr period of NARR analyses from 1979 through 2002, utilizing monthly averages of the data.

### b. Geographical regions of interest

The focus of this research is on North American basins with diverse climate regimes (Fig. 1b). In addition to the subbasins of the Mississippi River, two western U.S. basins are included. The Columbia River basin has

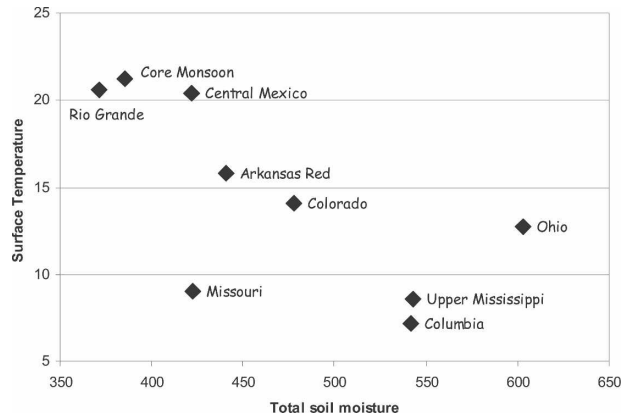


FIG. 2. Classification of the climate of each basin in Fig. 1b as a function of NARR annual mean values of surface air temperature (°C) and total soil moisture (mm).

orographically forced precipitation that is largest during winter with the resulting spring snowmelt. Basins affected by the North American monsoon are also included in this research. The core monsoon (Berbery 2001) is not strictly one basin, but the aggregation of several mountain basins directly influenced by the monsoon precipitation that drains toward the Gulf of California. The hydrological cycle of the semiarid Colorado River basin is affected by the monsoon regime during the warm season (Gochis et al. 2003) and by snow accumulation during the preceding cold season (Gutzler 2000). Other nearby basins potentially affected indirectly by the monsoon are considered, like the Rio Grande/Rio Bravo basin covering part of southern Texas and northern Mexico. The region identified as central Mexico, located in the eastern slopes of the Sierra Madre Occidental, is also inspected.

The basins have diverse climate regimes that are summarized in Fig. 2, where they are identified in terms of their mean annual soil moisture and surface temperature. The three warmer and drier basins are the Rio Grande, core monsoon, and central Mexico, in that order. At the other end, the upper Mississippi and Columbia are among the cooler and wetter basins, while the Missouri is relatively dry and cold. The three basins characterized by midrange surface temperature exhibit large differences in mean annual soil moisture, with the Ohio basin being the one with largest soil moisture and the Arkansas/Red the least.

### c. Water budgets

We consider the surface water budget equation,  $P - E - R - dW/dt - \text{Res} = 0$ , where  $P$  is the precipitation;  $E$  the evaporation;  $R$  the sum of surface and subsurface runoff;  $W$  the water content from snow accumulation,

soil moisture, and canopy water; and Res the residual. Although models are coded so that the residuals are zero, in practice this is not always true. Possible sources of imbalance are 1) additions of water during the data assimilation (including daily ingest of a snowpack analysis), 2) model errors, and 3) post processing issues. The last one includes the horizontal interpolations of the output from the model's native grid to a grid that can be employed by users. Regions of complex terrain, like the Columbia basin and the core monsoon, may be largely affected by the interpolations.

Precipitation in the NARR output fields is the precipitation that reaches the land surface after the effect of the precipitation assimilation in the atmospheric model of NARR, hence no additional term is needed in the water balance relation to reflect the assimilation of observed precipitation. On the other hand, an additional term should be included, one that represents the daily increment of surface water storage arising from the NARR assimilation of an external analysis of snowpack. Typically, the daily ingest of the snowpack analysis results in a positive increment to the water storage, as it tends to correct a tendency for overly rapid depletion of snowpack in the Noah LSM component of NARR (see the discussion in Mesinger et al. 2006). The term for the increment of surface water from the daily snow assimilation is not included in our diagnostics. Thus, evaporation may exceed precipitation over those basins that experience a significant amount of snowpack during the cold season and snowy mountainous areas may remain too wet even in the June–September (JJAS) mean values, as noticed in Fig. 3. (One cause of the early snowpack depletion bias in the Noah LSM has since been identified and the snowpack physics of the Noah LSM modified in NCEP operational models to reduce this bias by roughly half—see Ek et al. 2003.)

Table 1 presents the 24-yr mean water budget terms for all basins ordered by decreasing soil moisture content. Over the long-term average, precipitation at the surface should partition between evapotranspiration and runoff, and hence precipitation should exceed evapotranspiration. However, three basins (Colorado, Missouri, and core monsoon) depict evapotranspiration that exceeds precipitation by a small amount, about 0.1–0.2 mm day<sup>-1</sup>. For the first two basins, the imbalance can be attributed to the aforementioned snowpack updates during assimilation, although this is not the case for the core monsoon, where no winter snowpack is expected. The reasons for the core monsoon inconsistency are not identified yet.

In general, the approximate balance of the multiyear mean water budget in Table 1 is achieved primarily by  $P$  and  $E$ , with a smaller contribution from  $R$  and no

contribution (as expected over a multiyear period) from the local changes ( $dW/dt$ ). The Columbia and Ohio basins have the largest runoff contributions toward the balance. The magnitude of the residuals resembles that of the more recent years of the operational Eta Model products (Berbery et al. 2003; Luo et al. 2005). In the case of NARR, the monthly time series of the residuals are smaller than 0.5 mm day<sup>-1</sup> in magnitude during the 24-yr period (not shown). On the long-term average (Table 1), most basins have small residuals, of the order of 0.2 mm day<sup>-1</sup> or less, except for the Columbia and Colorado basins, which double that magnitude. The two basins are influenced by complex topography, which implies significant uncertainties even in the observed precipitation (Luo et al. 2005).

NARR has a smaller residual when compared to those of NCEP–National Center for Atmospheric Research (NCAR) and European Centre for Medium-Range Weather Forecasts (ECMWF) global reanalysis (e.g., Roads and Betts 2000; see also Roads et al. 2003). Notice that this is true despite that here we used significantly smaller-sized basins: our basins range from  $0.5\text{--}1 \times 10^6$  km<sup>2</sup> versus typical estimates for basins of about  $3 \times 10^6$  km<sup>2</sup>. Moreover, the results for complex terrain (e.g., core monsoon and Columbia) with residuals of 0.5 mm d<sup>-1</sup> have no equivalent comparison in global reanalysis that typically have difficulty in resolving the important regional circulation features of those basins. With a few exceptions, the order of the magnitude of the residuals listed in Table 1 is larger in basins with larger snowpack, thus indicating (as discussed earlier) that those residuals likely stem from the external water increment of the daily snowpack updates.

#### *d. Energy budgets*

The radiation and energy budget terms are presented in Table 2. The model time period for the radiation fluxes is the same as the surface turbulent fluxes, and for the output they are averaged in 3-h intervals. The order follows that of Table 1, that is, from largest to smallest soil moisture content. As shown in Fig. 2, the wetter basins tend to be cooler. The total cloud cover (in percent) also reflects a relation with soil moisture, with the wetter basins having more total cloud cover. The presence of clouds is an important element in the radiation budget, which is also summarized in Table 2. The net shortwave radiation is defined as  $SW = SW\downarrow - SW\uparrow$  where the arrows represent the direction of the flux. Likewise, the net longwave radiation is defined as  $LW = LW\downarrow - LW\uparrow$ . The total net radiation is defined as  $NR = SW + LW$ . The net shortwave radiation increases as basins with increasingly clear skies are considered because more downward shortwave radiation

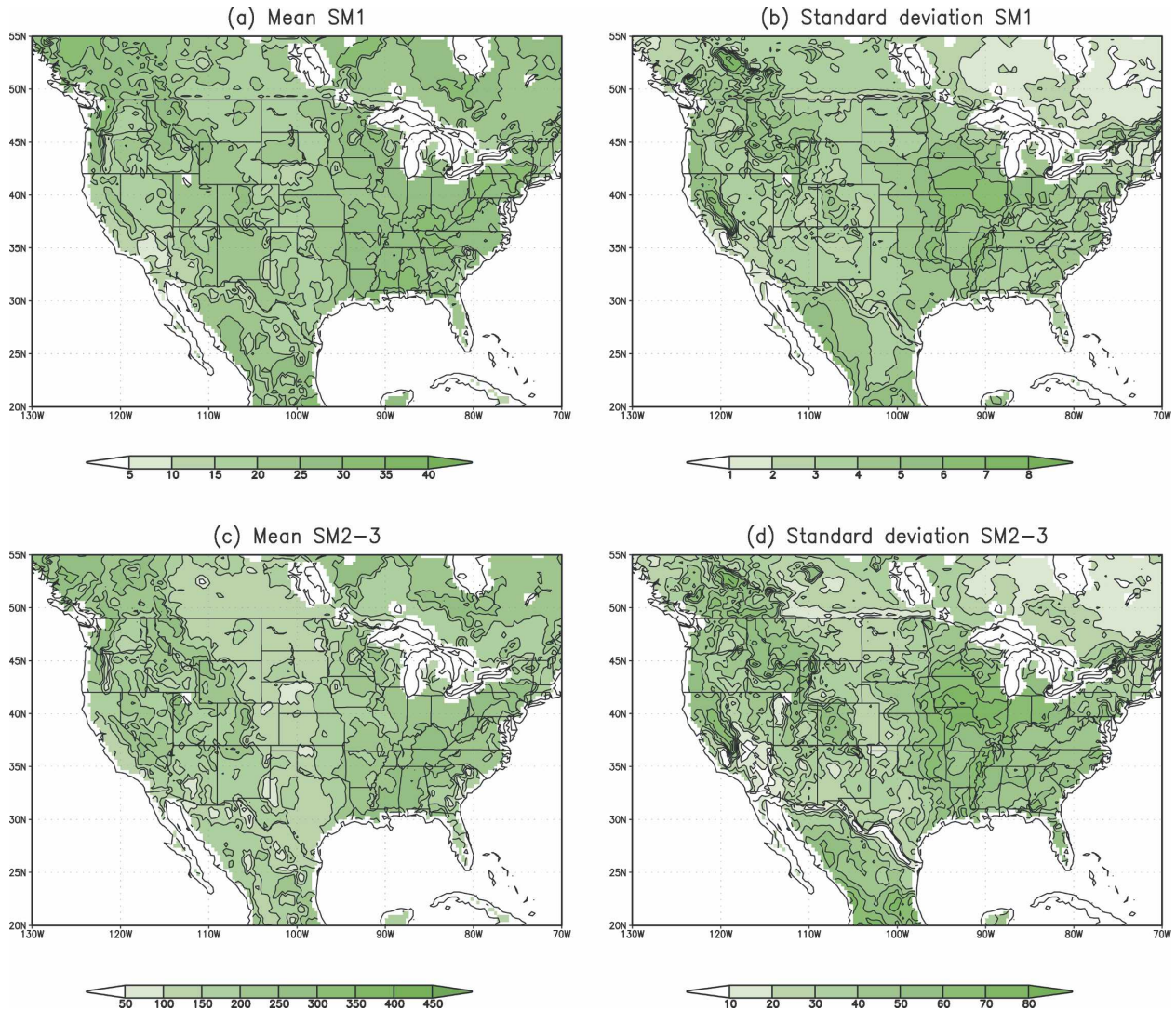


FIG. 3. The 1979–2002 JJAS (a) mean and (b) standard deviation of NARR soil moisture for the first layer (0–10 cm). The (c) mean and (d) standard deviation of soil moisture for layers 2–3 (10–100 cm). Units are  $\text{mm day}^{-1}$ .

reaches the surface. However, this is compensated by the larger loss due to the net longwave radiation, which also increases in magnitude as fewer clouds are present in the basins. Note that the total net radiation does not

show a clear relation to soil moisture or total cloud cover because of the loss of  $LW\uparrow$  to space and lesser downward emission by clouds. This will be discussed later for the warm season.

TABLE 1. Annual mean (1979–2002) water budget for all basins. TSM: total soil moisture,  $P$ : precipitation,  $E$ : evapotranspiration,  $N$ : surface and deep runoff,  $W$ : soil moisture plus snow water equivalent, Res: residual of the surface water balance. Units are  $\text{mm day}^{-1}$ .

Basin	Ohio	Upper Mississippi	Columbia	Colorado	Arkansas/Red	Missouri	Central Mexico	Core monsoon	Rio Grande
TSM	603.23	542.84	541.58	478.00	440.47	422.11	421.91	385.12	371.64
$P$	3.11	2.30	1.83	0.90	1.92	1.35	1.57	1.29	0.86
$E$	2.70	2.17	1.56	1.09	1.86	1.44	1.47	1.51	0.87
$R$	0.46	0.30	0.69	0.20	0.12	0.14	0.05	0.05	0.04
$dW/dt$	0.00	0.00	0.01	-0.01	0.00	0.00	0.00	-0.01	0.00
Res	0.05	0.18	0.42	0.39	0.06	0.23	-0.02	0.26	0.05
$E/P$ (%)	86.8	94.3	85.2	121.1	96.9	106.7	93.6	117.0	101.2

TABLE 2. Annual mean (1979–2002) surface energy budget for all basins. Ts: surface temperature, T Cl Cov: total cloud cover, SW↓: downward shortwave radiation; SW↑: upward shortwave radiation, LW↓: downward longwave radiation, LW↑: upward longwave radiation, NR: net radiation, LH: latent heat flux, SH: sensible heat flux, GH: ground heat flux, Res: residual of the surface energy balance, BR: Bowen ratio, EF: evaporative fraction. Units are  $W m^{-2}$  except for Ts, which is  $^{\circ}C$ , and total cloud cover, which is %.

Basin	Ohio	Upper Mississippi	Columbia	Colorado	Arkansas/Red	Missouri	Central Mexico	Core monsoon	Rio Grande
Ts	12.7	8.6	7.2	14.1	15.8	9.0	20.4	21.2	20.6
T Cl Cov	50.7	46.2	45.4	28.4	30.2	37.6	30.3	30.2	22.3
SW↓–SW↑	153.6	143.1	153.9	189.4	181.7	154.9	204.6	202.2	193.9
LW↓–LW↑	–58.7	–61.7	–81.9	–113.4	–90.4	–85.1	–105.1	–101.7	–109.9
NR	94.8	81.4	72.0	75.9	91.2	69.7	99.4	100.4	84.0
LH	–78.1	–62.7	–45.1	–31.6	–53.6	–41.5	–42.6	–43.7	–25.0
SH	–24.8	–25.3	–32.2	–53.9	–48.9	–36.6	–68.1	–68.2	–70.5
GH	–0.1	–0.2	–1.1	–1.3	–0.7	–1.0	–1.0	–0.5	–1.0
Res	–8.3	–6.9	–6.4	–11.0	–12.0	–9.5	–12.4	–12.0	–12.6
BR	0.32	0.40	0.71	1.71	0.91	0.88	1.60	1.56	2.82
EF	0.76	0.71	0.58	0.37	0.52	0.53	0.38	0.39	0.26

In wet basins, the net radiation is balanced primarily by the latent heat flux (LH), and secondarily by the sensible heat flux (SH). But in drier basins the sensible heat flux gains predominance over the latent heat flux. This is reflected in the Bowen ratio ( $BR = SH/LH$ ), which increases with basins of decreasing soil moisture content; the opposite occurs for the evaporative fraction [ $EF = LH/(LH + SH)$ ]. Notice that the ground heat flux is almost negligible (in the annual mean), while the residuals are primarily negative with typical values of around  $6\text{--}12 W m^{-2}$  in magnitude. The larger residuals of the surface energy balance are found in the southern part of the continent, particularly toward Mexico. To save computational time for use in operational models such as those at NCEP, the exact nonlinear and implicit form of the surface energy balance equation is linearized in the Noah LSM, for purposes of computational efficiency, which is a high priority for models used in daily operations. The linearization results in some modest energy balance residual. The residuals are similar to those found by Roads et al. (2003) for the whole Mississippi basin employing global reanalysis. However, the NARR results can be considered superior because the basins in our study are about  $5 \times 10^5 km^2$  and some of them over complex terrain, while the Mississippi basin as a whole is over  $3 \times 10^6 km^2$  over a comparatively flatter surface.

### 3. Land–atmosphere relationships

The diagnostics presented here are for JJAS, because in the cold season the surface and the boundary layer tend to become decoupled and the rainfall regimes depend more heavily on large-scale circulations (Dir-

meyer 2003). In evaluating the soil moisture distribution produced by a given land model in response to surface forcing, it is important to first characterize the climatology of that land model's soil moisture and then examine the departures (anomalies) of soil moisture from that climatology. In a given land model, the range of absolute value of soil moisture content depends on the maximum holding capacity (saturation), the field capacity (capacity when drainage from bottom of soil column essentially ceases), the soil moisture threshold below which transpiration starts to become soil moisture limited, and the amount of water that, although present, cannot be removed from the soil (wilting point). While the absolute values of soil moisture can be very different between land models even when provided the same surface forcing, the amplitude of their monthly/seasonal depletion (recharge) in warm/dry (cool/wet) periods can be quite similar, thus yielding similar monthly/seasonal surface fluxes (see Robock et al. 2003).

The representation of the soil moisture in NARR is constrained by the vertical resolution of the land surface model, which has four layers of depth: 0–10, 10–40, 40–100, and 100–200 cm. The 24-yr summer (JJAS) mean and standard deviation fields of soil moisture for NARR are depicted in Fig. 3 and taken as a reference for this study. This figure shows separately the shallow top layer (0–10 cm) and the combination of layers 2 and 3 (10–100 cm). (Note the different color scale for each panel of Fig. 3.) Figures 3a,c show that, in general terms, and not considering the smaller-scale structure, soil moisture tends to be high over the southeastern and northwestern parts of CONUS, while lower values are noticed toward the center. The spatial structure of the mean fields for the top and deeper layers is similar,

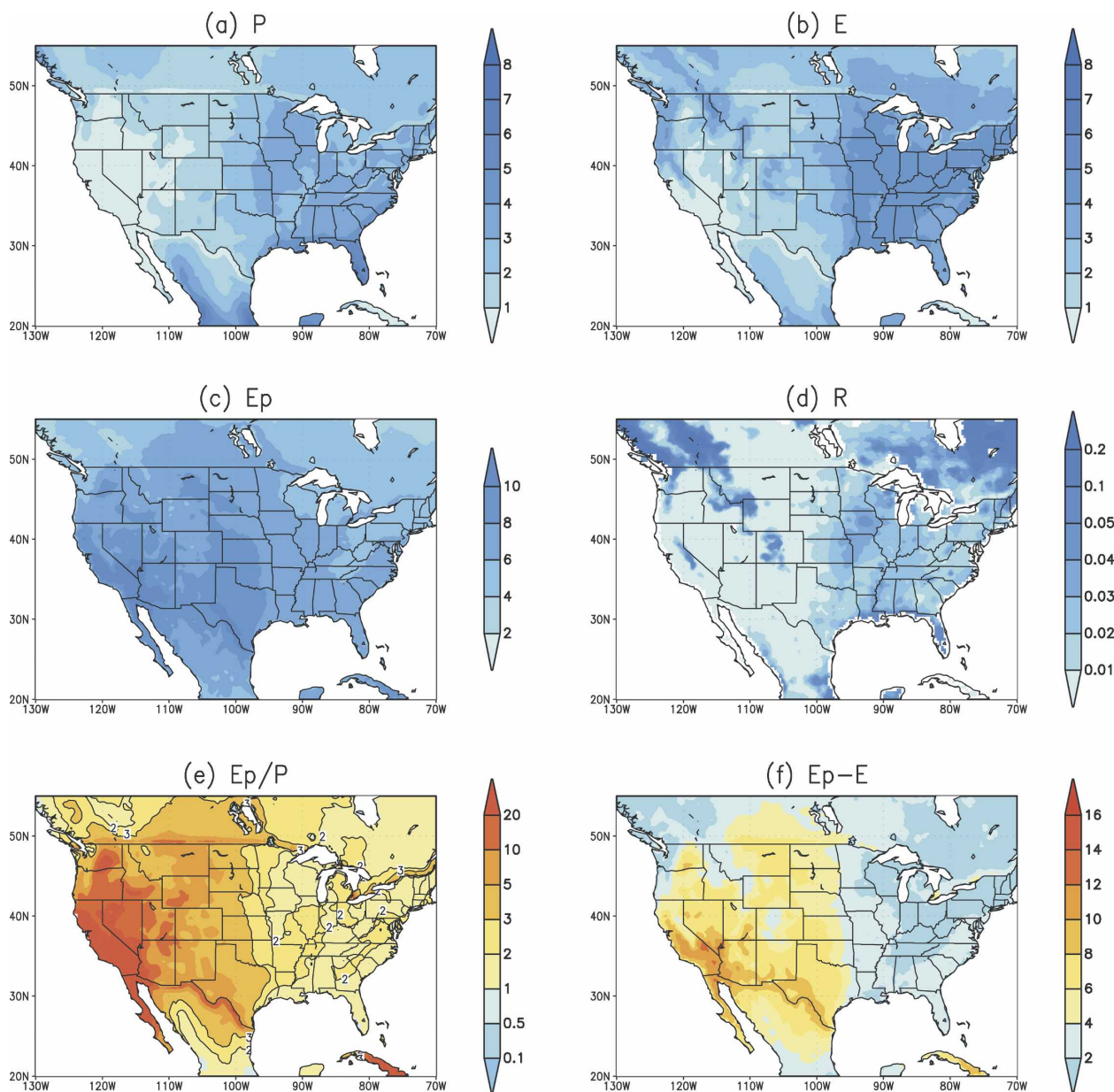


FIG. 4. The summer mean (JJAS) fields of (a) precipitation, (b) evapotranspiration, (c) potential evaporation, (d) total runoff (surface runoff plus baseflow runoff), (e) ratio between potential evaporation and precipitation, and (f) difference between potential evaporation and evapotranspiration. Units for (a)–(d) and (f) are  $\text{mm day}^{-1}$ ; (e) has no units.

although the magnitudes differ, with the exception of the core monsoon region in northwestern Mexico. According to Figs. 3b,d, the largest variability of soil moisture, as represented by its standard deviation, is found over the regions of largest soil moisture content (Figs. 3a,c). The eastern United States is an exception, as the largest variability is found toward the northern Great Plains (centered approximately over Iowa) while the largest mean values tend to be in the southern portion (over Mississippi and Alabama).

Some discontinuities along the U.S.–Canada and U.S.–Mexico borders become evident in some panels of Fig. 3 (and Fig. 4 as well). These can be attributed to the vast discontinuity across the borders in the spatial density of the rain gauge observations that were available to NCEP to construct the gridded precipitation analyses that were assimilated. As precipitation is assimilated, the discontinuity may be transferred to other variables such as soil moisture and evaporation, as evident in Fig. 4. Of all the basins considered, the Rio

Grande is the one that may be more exposed to these uncertainties, as it straddles the U.S.–Mexico border.

*a. Interplay between potential evaporation and precipitation*

Soil moisture memory can be an important source of long-term weather predictability for some midlatitude continental regions (Koster et al. 2000). The ratio of potential evaporation to precipitation ( $E_p/P$ ) is a useful diagnostic of soil moisture memory (Delworth and Manabe 1988, 1989). Large values of the ratio imply large potential for evapotranspiration and/or little precipitation, meaning that there will be ample energy to evaporate soil moisture anomalies, and thus, their persistence will be low. On the other hand, small values of the ratio suggest that there is abundant soil water (because of the precipitation) but not enough energy to evaporate it all, and evaporation anomalies will be less dependent on soil wetness and more dependent on anomalies in available energy (e.g., from variations in cloudiness, air temperature, wind speed). In these cases, evapotranspiration is not far different from the potential evaporation, and runoff begins to act to remove water from the system. Additionally, in this paper we use the difference between potential evaporation and evapotranspiration ( $E_p - E$ ) as a measure of water and energy availability; regions with large values of  $E_p - E$  imply abundance of energy to evaporate (but not enough availability of water); while values close to zero imply regions of abundance of water sufficient to satisfy reasonably well the evaporative demand.

The above diagnostics depend on the interplay between precipitation, evapotranspiration and potential evaporation, which will be discussed further using Fig. 4. The figure shows the mean summer fields of the major terms in the water balance ( $P$ ,  $E$ ,  $R$ ), as well as  $E_p$  and its comparison to  $P$  and  $E$ . Figure 4a shows the familiar precipitation pattern during summer, with a west-to-east gradient with larger values toward the eastern half of the United States; a second maximum can be found over the western slopes of the Sierra Madre Occidental in western Mexico. The evapotranspiration (Fig. 4b) follows a similar pattern, although large values are also noticed near the Columbia basin. Notice that, in contrast, the potential evaporation (Fig. 4c) is largest over the southwestern United States, resembling the typical structure of the surface air temperature field and shortwave radiation field (see, e.g., Berbery et al. 2003, their Fig. 9).

Following Delworth and Manabe (1988, 1989), the very dry regions of the western part of the continent exhibit large  $E_p/P$  (see Fig. 4e), indicating that there is large potential evaporation but with limited water sup-

ply (small precipitation). In these regions, soil moisture anomalies are rapidly damped by the high  $E_p$  and  $E$ , and thus the time scale of soil moisture anomalies are usually quite short, because there is plentiful energy but limited water supply and stored soil moisture is quickly removed. Likewise, Fig. 4f shows that the same regions have the largest differences between the potential evaporation and the actual evapotranspiration ( $E_p - E$ ). Both in Figs. 4e and 4f, the large values extending along the U.S.–Mexico border are likely due to the discontinuities in some surface fields discussed earlier.

Wet regions have small  $E_p/P$  (Fig. 4e) and  $E_p - E$  (Fig. 4f). Here, frequent runoff is required to balance the hydrologic budget, and by this mechanism the decay time scales of soil moisture are substantially shortened (Delworth and Manabe 1988). The runoff field (Fig. 4d) is precisely largest in areas where the ratio  $E_p/P$  and  $E_p - E$  are smallest. The smaller values are found over the Ohio, upper Mississippi, and Columbia basins.

*b. Relation between precipitation and soil moisture*

In the absence of sublimation from the snowpack, the three components of total surface evaporation are: 1) direct soil evaporation from the top soil layer, 2) transpiration from the root zone, and 3) evaporation of dewfall or intercepted precipitation on the vegetation canopy (Ek et al. 2003). In NARR the root zone is 3 layers deep (1 m) for all nonforest vegetation classes and 4 layers deep (2 m, entire model soil column) for all forest vegetation classes. We expect that transpiration is the main source of moisture from the deeper soil column to the boundary layer in regions of nonsparse vegetation and that direct soil evaporation from the first soil layer dominates the total evaporation in vegetation-sparse regions. Unfortunately, the diagnostic variables in the NARR dataset do not provide the three separate evaporation components to illustrate this.

Figure 5a presents the correlation field between the top-layer soil moisture and precipitation. Correlation values above 0.20 in magnitude are statistically significant at the 95% level. For the top layer, positive correlations are apparent everywhere over North America, with values exceeding 0.5 over the majority of the CONUS, and exceeding 0.6 (and as high as 0.8) in regions where the soil is not too wet (see Fig. 3). Given that the top layer is relatively shallow, directly exposed to the precipitation, and has relatively short drying time scales, such consistently high positive correlation is expected and we believe it reflects primarily the one-way direct effect of the precipitation on the top-layer soil moisture. Nonetheless, Fig. 5a also shows different degrees of correlation, depending on the geographical lo-

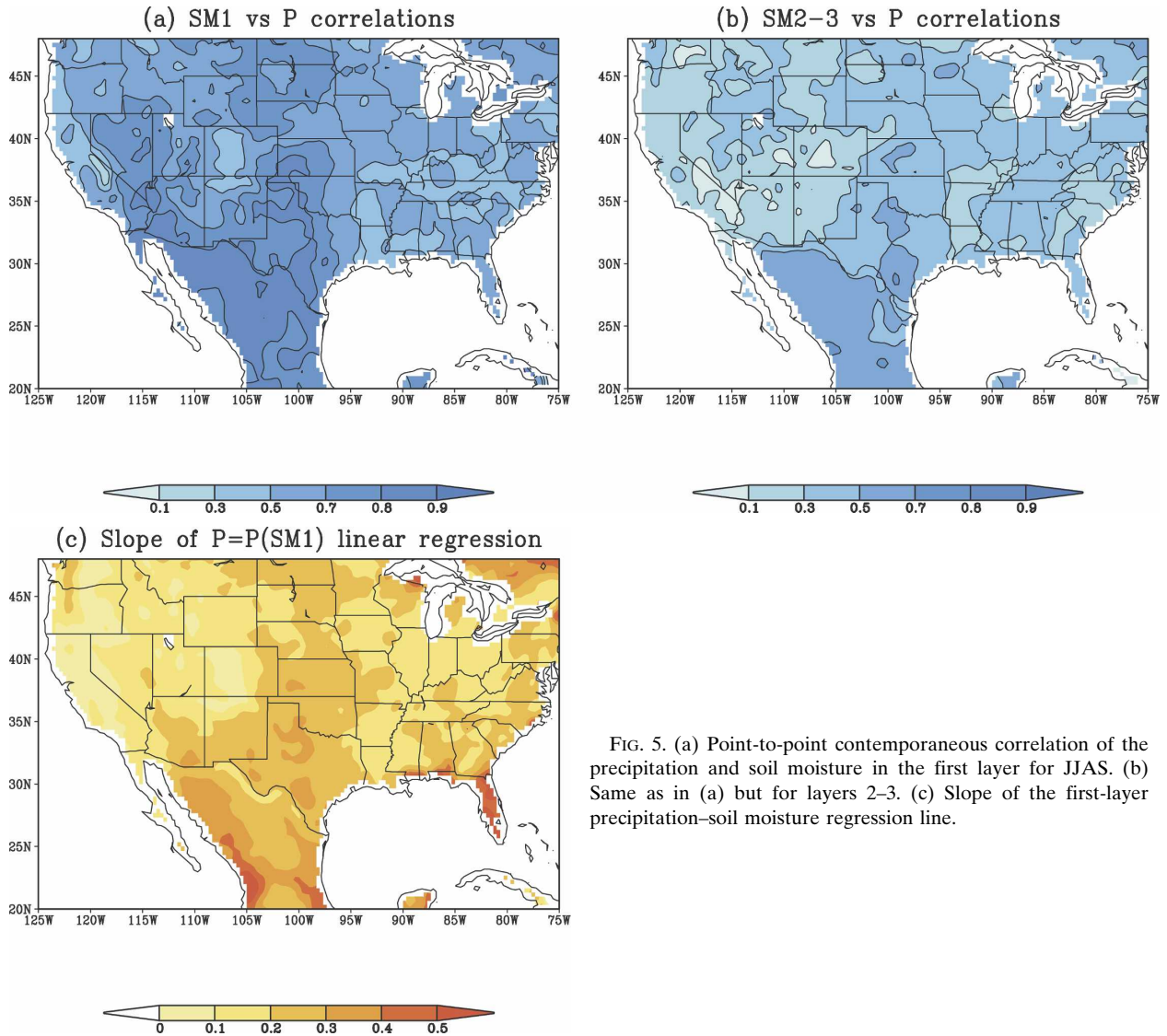


FIG. 5. (a) Point-to-point contemporaneous correlation of the precipitation and soil moisture in the first layer for JJAS. (b) Same as in (a) but for layers 2–3. (c) Slope of the first-layer precipitation–soil moisture regression line.

cation, with other elements like evaporation affecting the top-layer soil moisture pattern in the wetter areas that can sustain evaporation over longer periods.

Of greater interest is Fig. 5b, which shows the correlation field between precipitation and deeper soil moisture (layers 2–3). Compared to Fig. 5a, correlations are smaller (and only small regions exceed 0.5), with a large difference apparent over the southwestern United States (particularly over the Colorado River basin) where the correlations in Fig. 5b are notably lower than in Fig. 5a. It is expected that the warm-season evapotranspiration over this arid region will be dominated by bare-soil evaporation from the first layer, as it is anticipated that the transpiration from the deeper soil layers to be rather small given the spatially sparse vegetation cover over this arid region (Fig. 1a).

The link between precipitation and soil moisture in the deeper layers 2–3 should reflect (slower) processes that result when precipitation percolates to the deeper layers. In the land–atmosphere system this deeper water can later transpire to the atmosphere, providing an additional (albeit delayed) source of moisture for precipitation, which may be better reflected in lagged correlations. On the other hand, simultaneous (lag 0) correlations tend to be higher when top-layer soil moisture is considered. We later present results for lagged correlations in section 3d.

The regions in Fig. 5a with stronger precipitation–near-surface soil moisture correlations are also the ones with higher sensitivity (larger values of the slope of the linear regression analysis) as seen in Fig. 5c (a similar analysis for the deeper layers, not shown, results in

smaller slopes everywhere, likely reflecting the slower times scales). Large regression slopes are found over the southern United States and Mexico, and small values (less sensitivity to changes) are noticeable over the wetter regions like the Ohio and Columbia basins. These basins have lower correlation and sensitivity because they have more moisture available for evaporation than energy to achieve the evaporation. It is speculated that over such wetter basins, it takes larger anomalies of soil moisture to result in meaningful anomalies of surface evaporation, boundary layer moisture, and cloudiness. In addition, the eastern Mississippi subbasins are more influenced by the large-scale low-level moisture flux from the Gulf of Mexico, thus clouds and precipitation on this region relate better to convergence of moisture flux than to surface moisture flux and soil moisture (as suggested also in Berbery et al. 2003).

### *c. Soil moisture links to the surface and atmosphere conditions*

The soil moisture–atmosphere coupling is a two-way interaction. Soil moisture, especially in the top soil layer, responds directly to precipitation. In the NARR, the assimilation of observed precipitation, converted to atmospheric latent heating rates and vertical motion (Lin et al. 1999), ensures that the model precipitation is close to the input precipitation analyses. Precipitation and the cloud radiative forcing, which affect the surface energy budget, are linked by the model physics. Additionally, the evaporation of falling precipitation modifies the boundary layer. The surface evaporative fraction (EF) depends on soil water, as well as water in the skin reservoirs (canopy interception and dew), and in turn the EF modifies the boundary layer structure and boundary layer cloud cover.

To examine the relation in NARR between soil moisture on the one hand and other surface and lower-atmospheric variables on the other, we present in Figs. 6–8 the anomaly scatterplots of the summer mean (JJAS) of selected variables against first-layer soil moisture. For these figures, we derived area-averaged variables for all basins and removed the effect of seasonal variations by subtracting the mean annual cycle from all the time series. The Columbia basin represents a wet and cold climate, while the core monsoon represents the driest and warmest region. In the Mississippi basin, the Arkansas/Red subbasin is drier and warmer than the Ohio subbasin. The complete results for all basins are presented in Table 3 and will be discussed as a summary at the end of this section.

Figure 6 shows the relationship between net shortwave radiation, net longwave radiation, and surface

temperature and near-surface soil moisture. The shortwave and longwave impacts of the cloud field on the radiation budget have been recognized as the major source of uncertainty in numerical models (Betts and Viterbo 2005; Stephens 2005). Soil moisture and net shortwave radiation exhibit an inverse correlation (Figs. 6a,b) that can be related to changes in cloud coverage, as soil moisture and cloud cover generally increase together (see Figs. 8c,d, described later), and increased cloud cover reduces the amount of shortwave radiation that reaches the surface. The strongest negative correlation for soil moisture and net shortwave radiation corresponds to the core monsoon, while the weakest is found for the Ohio basin. The Arkansas/Red and Columbia basins are somewhere in between. In addition, the core monsoon net shortwave varies most with soil moisture changes (as represented by the slope of the regression line), while the Ohio and Columbia basins vary least. The net longwave radiation increases with increasing soil moisture (Figs. 6c,d). This increase is related to a smaller upward longwave radiation and the reduced surface temperature with increasing soil moisture (Figs. 6e,f), but also to an increase of the downward longwave radiation due to the larger emission from the greater cloud coverage (Figs. 8c,d, discussed later), higher humidity, and lower cloud base (Figs. 8a,b described later) associated with higher soil moisture. Notice also that the dispersion along the regression line is smaller for the net longwave than for the net shortwave radiation, suggesting a tighter coupling between soil moisture and net longwave radiation. Again, the larger correlations correspond to the drier basins (core monsoon and Arkansas/Red).

The scatterplots for the total net radiation (SW + LW) are not shown, but the results are summarized next. The changes in net shortwave radiation and net longwave radiation with changes in soil moisture tend to be of opposite sign and hence tend to cancel each other, so that the change in total net radiation can increase or decrease modestly with increasing soil moisture, depending on which radiation component is larger in magnitude. Of the four basins discussed here, the Arkansas/Red and Columbia reveal an increase of net radiation with increased soil moisture, consistent with Eltahir's (1998) results suggesting that net radiation is higher when the soil is relatively wet. In the other two basins, core monsoon and Ohio, the net longwave effect is larger than the net shortwave, resulting in a reduction of net radiation with increased soil moisture.

The relation between near-surface soil moisture and surface energy fluxes shown in Fig. 7 has been discussed in earlier articles (Betts and Ball 1998; Betts and Viterbo 2005; Betts 2007). In all basins, increases of soil

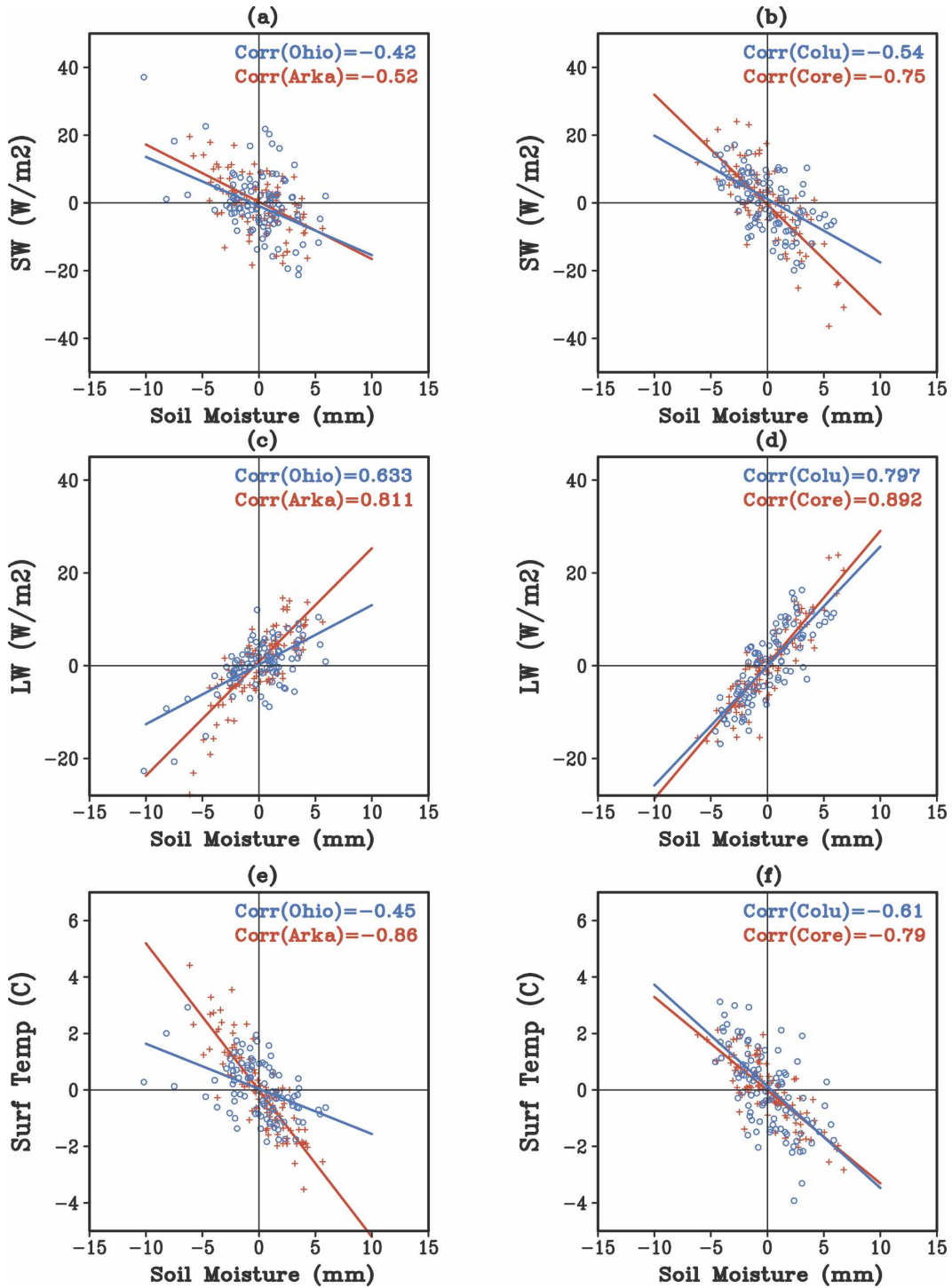


FIG. 6. The summer mean (JJAS) scatterplots of anomalies of area-averaged variables vs soil moisture in the first layer for four basins: (a) Ohio and Arkansas/Red and (b) Columbia and core monsoon net shortwave radiation; (c) Ohio and Arkansas/Red and (d) Columbia and core monsoon net longwave radiation; and (e) Ohio and Arkansas/Red and (f) Columbia and core monsoon surface temperature.

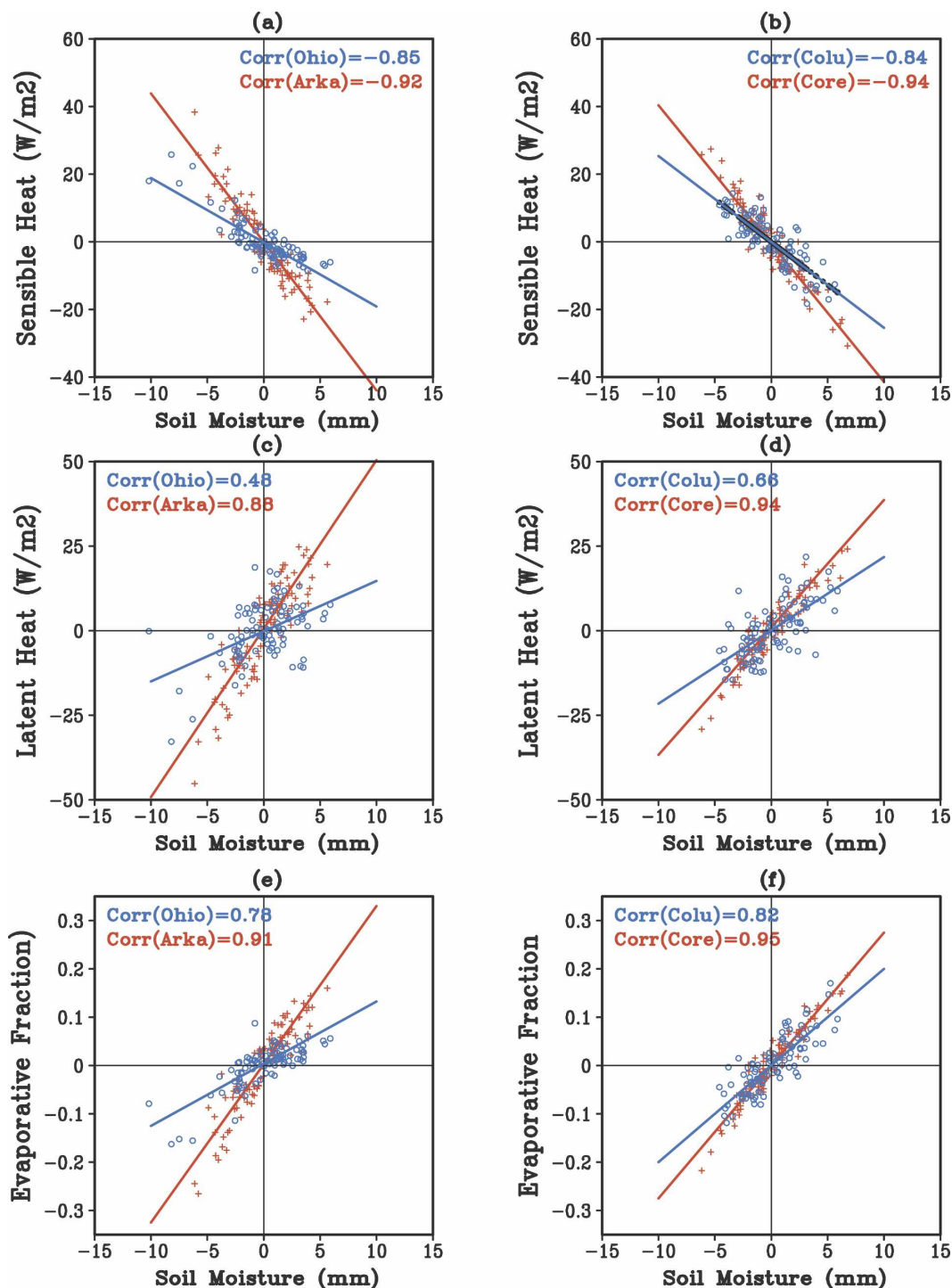


FIG. 7. Same as in Fig. 6 but for (a), (b) sensible heat flux; (c), (d) latent heat flux; and (e), (f) evaporative fraction.

moisture correspond with cooling of the surface, as noted in decreases of sensible heat flux (Figs. 7a,b), and with increases of evaporation, as measured by the latent heat flux (Figs. 7c,d). The strength of the correla-

tion depends on the amount of soil moisture, with drier basins (core monsoon and Arkansas/Red) having larger correlations than wetter ones (Columbia and Ohio). Also, the sensitivity to changes in soil moisture (the

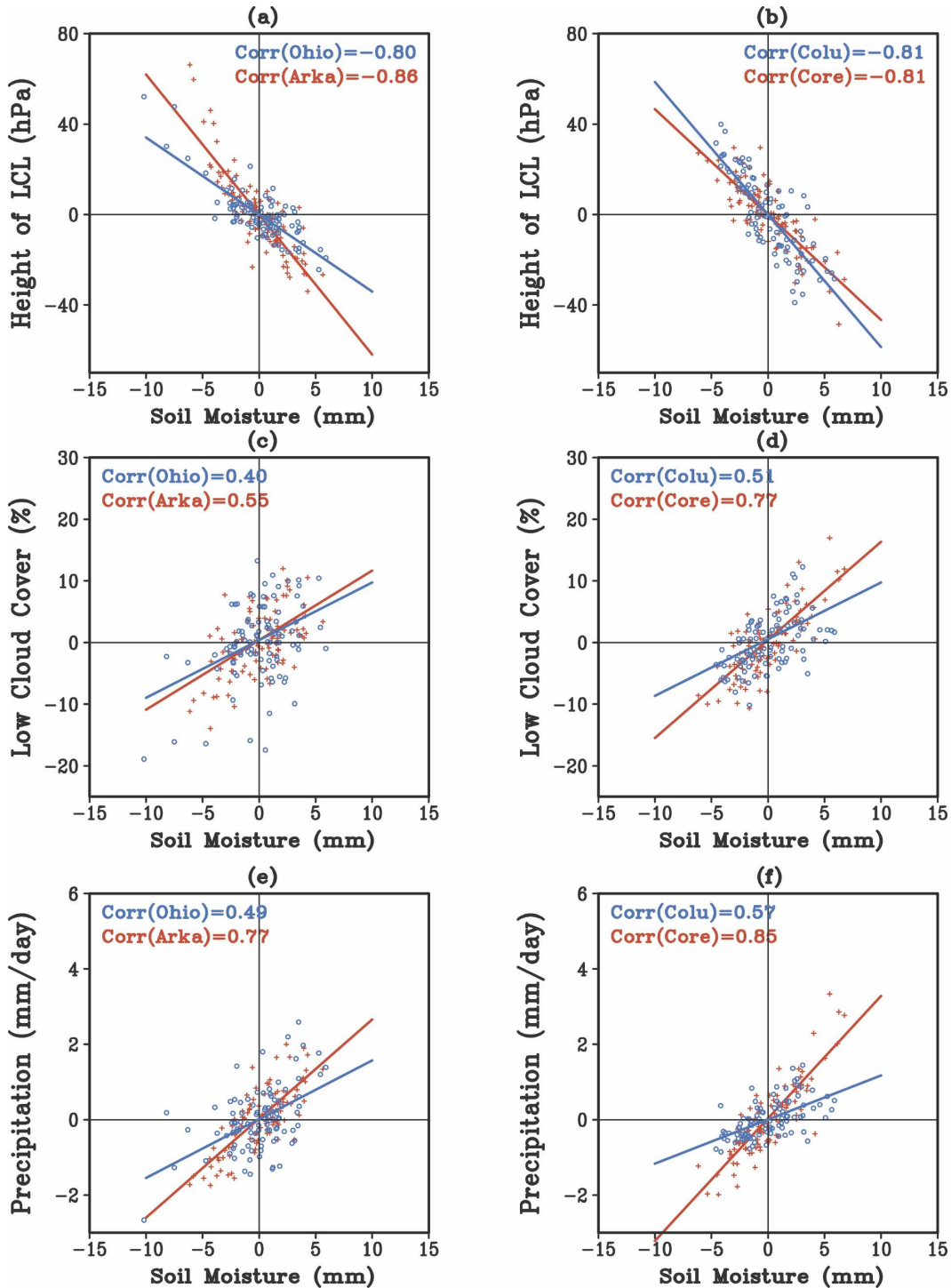


FIG. 8. Same as in Fig. 6 but for (a), (b) height of the LCL; (c), (d) low cloud cover; and (e), (f) precipitation.

slope of the regression line) is more noticeable in the drier basins where surface fluxes tend to vary considerably with soil moisture. Conversely, the slope is smaller in wetter basins, indicating that surface energy fluxes are not as responsive to changes in soil moisture

as in the drier western basins, owing to the available energy generally being less than the available water in the wetter basins. One factor contributing to the higher available water in the wetter basins is the more dense vegetation cover (Fig. 1a), which can better draw upon

TABLE 3. These are JJAS correlations between first-layer soil moisture and surface variables. LCDC: low cloud cover, LCL: lifting condensation level; see Table 2 for definition of other symbols.

	<i>P</i>	Ts	NR	SW	LW	LH	SH	EF	LCDC	LCL
Core monsoon	0.86	-0.79	-0.20	-0.76	0.89	0.95	-0.94	0.96	0.78	-0.82
Rio Grande	0.85	-0.83	0.50	-0.72	0.86	0.97	-0.95	0.98	0.76	-0.85
Central Mexico	0.84	-0.92	0.14	-0.73	0.90	0.91	-0.98	0.97	0.80	-0.91
Arkansas/Red	0.78	-0.87	0.44	-0.53	0.81	0.88	-0.93	0.92	0.56	-0.86
Missouri	0.75	-0.76	0.58	-0.65	0.89	0.87	-0.91	0.91	0.67	-0.89
Colorado	0.73	-0.35	0.84	-0.61	0.84	0.91	-0.78	0.92	0.69	-0.80
Upper Mississippi	0.62	-0.57	0.18	-0.45	0.77	0.75	-0.87	0.85	0.40	-0.85
Columbia	0.58	-0.61	0.48	-0.54	0.80	0.67	-0.84	0.83	0.52	-0.82
Ohio	0.50	-0.46	-0.09	-0.42	0.63	0.48	-0.85	0.79	0.40	-0.80

the deeper soil moisture in the root zone to sustain evapotranspiration in the face of decreasing near-surface soil moisture. As shown in Figs. 7e,f, the higher soil moisture of the wetter basins with more vegetation cover manifests a relatively high evaporative fraction (larger surface latent heat flux and smaller surface sensible heat flux).

Betts et al. (1996, 1998), Betts and Viterbo (2005), and Betts (2007) have shown that the boundary layer depth is closely linked to soil moisture, or to the availability of water vapor for evaporation, especially where the clouds modify the shortwave and longwave radiative flux at the surface. The reduced sensible heat flux leads to reduced warming of the boundary layer and reduced entrainment at the top of the boundary layer, while the larger evaporation (Figs. 7c,d) increases the humidity of the boundary layer. Figures 8a,b show that higher soil moisture is therefore associated with a lower LCL, and higher low cloud cover, as depicted in Figs. 8c,d. Over the Columbia basin and eastern half of the Mississippi basin, low cloud cover and soil moisture are only weakly coupled, but in the central United States and Mexico the boundary layer processes and clouds and soil moisture are more tightly coupled. Figures 8e,f show the positive correlation between precipitation and near-surface soil moisture, as in Fig. 5a.

The NARR provides a reasonable picture of how soil

moisture variations relate to the surface radiation balance, the surface energy balance, the boundary layer conditions, the cloud fields, and the precipitation over North American basins. These relationships are summarized in Table 3. The correlations are significant at the 95% level, and even most are at the 99% level for correlation values of 0.20 and 0.2612, respectively. Therefore, except for the net radiation in some basins, most correlations are robust above the significance level. The results for all basins confirm that, in general, the wetter the basin, the lower the correlations. The basins with higher correlations between soil moisture and precipitation are also most likely to have higher correlations with the other variables, and vice versa.

A similar analysis for the total soil moisture (Table 4) shows a decrease in the correlation magnitudes for all variables indistinctly of the basin characteristics. Simultaneous correlations, although they are from monthly averages, may not reflect the delay that can result from the process of infiltration and later transpiration. A follow-up study is planned to investigate the time scales that may best reflect the interactions between the variables and the deeper soil layers. To highlight the importance of the soil moisture depth, consider the early discussion about the importance of intermediate values of soil moisture (not too dry, not too wet) for better links among variables. This is because dry basins have

TABLE 4. Same as in Table 3, but for the total soil moisture.

	<i>P</i>	Ts	NR	SW	LW	LH	SH	EF	LCDC	LCL
Core monsoon	0.60	-0.78	-0.13	-0.53	0.63	0.86	-0.85	0.88	0.57	-0.54
Rio Grande	0.54	-0.74	0.46	-0.46	0.60	0.86	-0.85	0.87	0.54	-0.58
Central Mexico	0.61	-0.78	0.05	-0.48	0.67	0.86	-0.85	0.89	0.58	-0.72
Arkansas/Red	0.40	-0.68	0.56	-0.19	0.52	0.80	-0.79	0.76	0.21	-0.58
Missouri	0.32	-0.47	0.59	-0.32	0.60	0.76	-0.80	0.77	0.31	-0.54
Colorado	0.14	-0.46	0.58	-0.03	0.31	0.78	-0.81	0.80	0.20	-0.27
Upper Mississippi	0.39	-0.51	0.28	-0.28	0.61	0.73	-0.80	0.80	0.24	-0.71
Columbia	0.18	-0.41	0.60	-0.21	0.50	0.76	-0.91	0.86	0.16	-0.51
Ohio	0.30	-0.44	0.05	-0.26	0.50	0.57	-0.83	0.79	0.27	-0.62

sparse vegetation and the total surface evaporation is dominated by direct evaporation, which is taken only from the surface soil layer. But the first soil layer is thin (0–10 cm) and has relatively little soil moisture holding capacity. Once a precipitation event ends in a dry basin, the elevated surface evaporation is short lived and cannot last long enough to impact a subsequent precipitation event. In contrast, in wet basins with substantial nonsparse vegetation cover, the vegetation can draw upon a deep root zone that has a high soil moisture holding capacity. In such basins the total surface evaporation is dominated by the plant transpiration, which does not begin to feel soil moisture limited until the vertically averaged soil moisture of the entire root zone drops significantly below the soil moisture threshold at which transpiration begins to feel stress. Therefore, achieving significant decrease in transpiration—enough to impact a subsequent precipitation event—requires a very large negative precipitation anomaly over a rather long period.

#### d. Implications for the predictive skill of precipitation

The previous subsection presented the correlations and degree of correspondence in the NARR between top-layer soil moisture and several near-surface atmospheric variables, surface latent and sensible heat flux, surface radiative fluxes, and precipitation. The question remains as to what extent soil moisture anomalies contribute to the predictive skill of precipitation on month-to-seasonal time scales.

The persistence of soil moisture anomalies could serve as a useful signal in predictability assessment if such persistence is manifested in future anomalies in atmospheric conditions. Under certain assumptions (Delworth and Manabe 1988; see also comments in Liu and Avissar 1999), 1-month lag autocorrelation values can be converted to anomaly decay times; for example, following Delworth and Manabe (1988), autocorrelations of 0.4, 0.6, and 0.8 correspond to  $e$ -folding times of 1.1, 2.0, and 4.5 months, respectively, implying that larger autocorrelations correspond to longer time scales of the soil moisture anomalies.

The 1979–2002 JJAS 1-month lag autocorrelation of soil moisture for the first meter (soil layers 1–3) is depicted in Fig. 9a. Positive values ranging between 0.6 and 0.9 indicate that anomalies of deep soil moisture persist on multimonth time scales. The larger values are found over the eastern and western United States. In the central region, lower values in the 0.6–0.7 range are noticed. The pattern is consistent with the previous argument that wet and dry areas tend to have larger persistence, but in fact this information does not necessar-

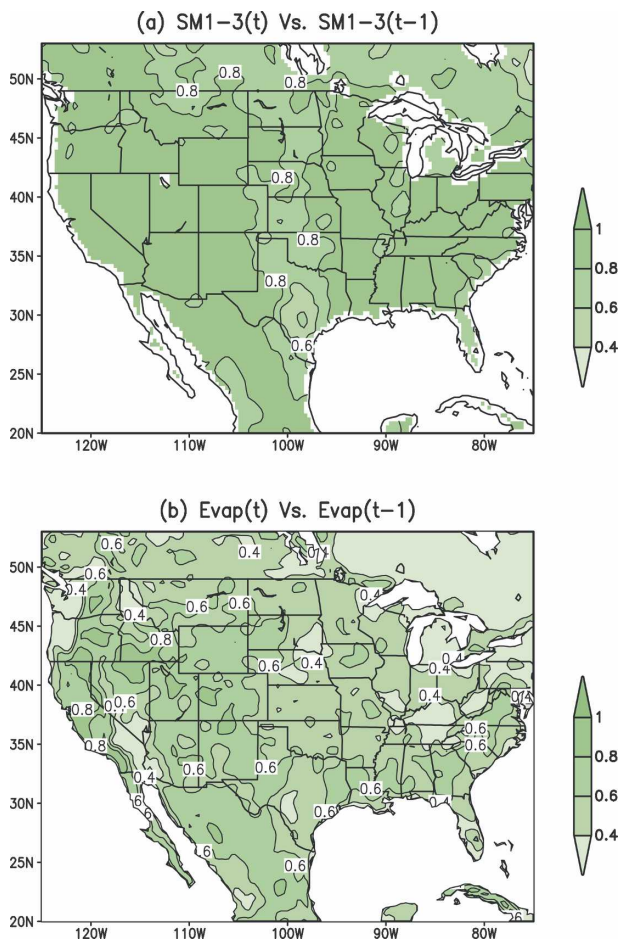


FIG. 9. (a) The 1-month lag autocorrelation field for soil moisture in layers 1–3 (0–100 cm). Each summer (JJAS) month's soil moisture is correlated with the preceding month's soil moisture. (b) Same as in (a), but for evapotranspiration.

ily translate into useful information to improve the predictive skill if the correlations among variables are low and if the soil moisture anomaly does not affect the evaporation. In contrast to soil moisture, the 1-month lag precipitation autocorrelation (not shown) has noticeably lower values, typically of the order of 0.2–0.4. The longer time scales for soil moisture autocorrelations are consistent with the land acting as an integrator of shorter-term precipitation events that produces a lower-frequency signal in soil moisture (Delworth and Manabe 1988). Soil moisture anomalies are not relevant if they do not dominate over other surface conditions that regulate evapotranspiration, for example the nonsoil moisture factors in the canopy conductance that constrain the transpiration, or the available energy. For this reason, it is also of interest to present the autocorrelation of evapotranspiration (Fig. 9b), which, unlike soil moisture, shows lower values in very wet

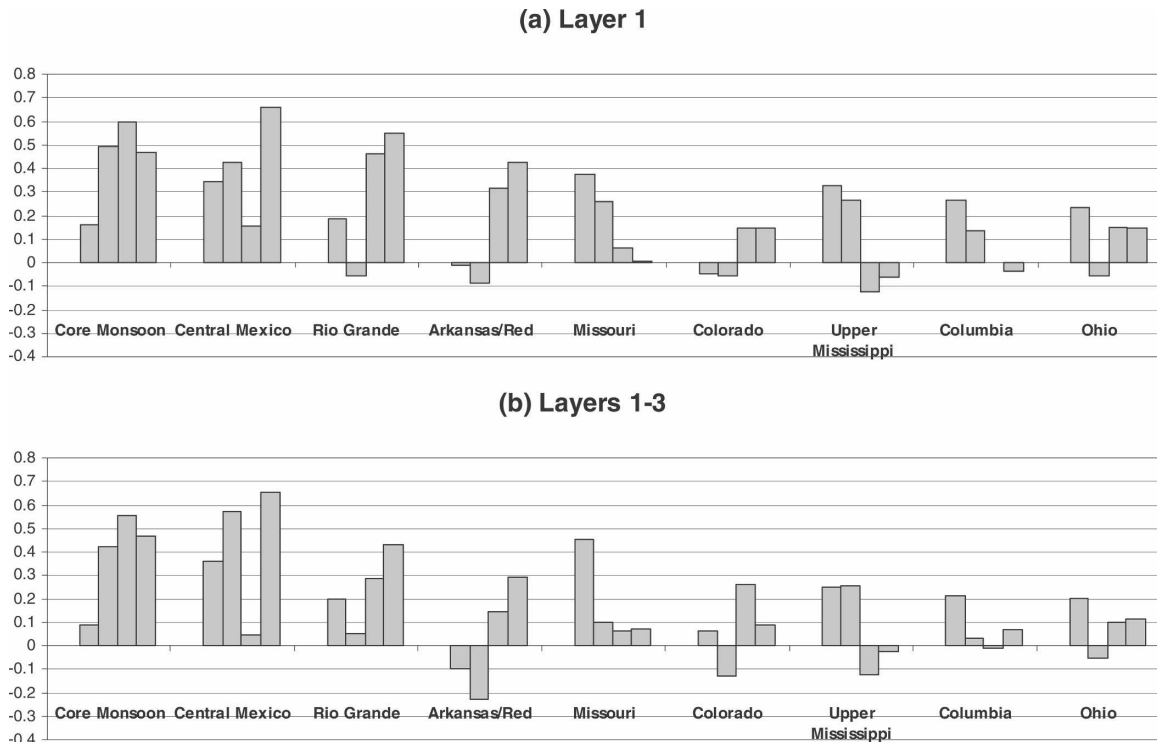


FIG. 10. Bar graph showing for each basin the correlation coefficients of soil moisture vs 1-month lag precipitation for each month (JJAS): (a) for the 0–10-cm depth (first soil layer) and (b) the 0–100-cm depth (top three soil layers). Values greater than 0.4 are above the 95% confidence level.

regions (the regions where evapotranspiration is close to the potential evaporation). In a similar manner, the dry region over the Colorado basin also depicts lower evapotranspiration autocorrelation values. These results suggest that the high persistence noticed in Fig. 9a for soil moisture does not necessarily translate into correspondingly significant persistence or magnitudes of anomalies of evapotranspiration, and thus such persistence of soil moisture anomalies has less effect on atmospheric conditions than might be anticipated.

So far, the analysis here has given background information for the hypothesis that soil moisture conditions can be favorable for feedbacks to exist and thus enhance predictive skill of precipitation in certain regions. Figure 10 presents, for each basin, the strength of the deep and shallow soil moisture–precipitation links for 1-month lags. As defined here, the strength of the link is given by the correlation of precipitation ( $P_t$ ) with the preceding month's soil moisture ( $SM_{t-1}$ ). The subscript “t” refers to time at monthly intervals. The index 1 or 1–3 following SM refers to the layers of soil moisture that were considered: SM1 denotes the soil moisture in the top layer (10 cm), while SM1–3 denotes the soil moisture in the top 3 layers (0–100 cm). For each basin, Fig. 10 shows four bars depicting the correlation for

each of the summer months (June–September). Correlations larger than 0.4 are significant at the 95% level. The hypothesis behind this analysis is that if a region does not exhibit strong correlation values, then it is unlikely that feedbacks between precipitation and soil moisture will develop. Therefore, these regions would not support a mechanism by which prediction from soil moisture could be expected. It is important to emphasize that strong lag correlations do not necessarily mean a measure of predictability, as the two variables may be responding to a large-scale pattern at lower frequencies.

Figure 10a shows an inverse dependence of the correlation with the degree of climatological soil moisture dryness. Notice that the values tend to follow the order of the correlations discussed in Table 3. Some regions, like the core monsoon and central Mexico, have higher precipitation correlations from the surface conditions in several summer months. Others, like the Arkansas/Red and Rio Grande achieve significant correlations only in late summer. No meaningful correlations from the land surface are found in the wetter basins, including the upper Mississippi, Ohio, and Columbia basins. The Colorado basin also ranks among those with poor link between soil moisture and precipitation, although it is

close to the drier basins. According to Fig. 10b, when considering deeper layers the correlations are slightly reduced, not increased. This may be the result of deeper layers having an effect over still longer time scales, rather than in the 1-month lag correlations. In addition, while the relation between land and near-surface atmospheric variables (as well as moisture persistence) tends to be rather uniform within a season (not shown), the lag soil moisture–precipitation correlation is not. The dependence of these terms with the time scales and depth will be a subject of future work.

#### 4. Summary and concluding remarks

The North American Regional Reanalysis (NARR) was employed to investigate the relations between near-surface soil moisture and other land surface variables and near-surface atmospheric conditions to better understand the relations between soil moisture and precipitation and the potential implications for the precipitation's predictive skill.

The NARR has assimilated a diverse mix of observations, including precipitation, resulting in a consistent dataset that can be employed in a wide range of hydroclimate studies. The reliability and strength of the land–atmosphere interactions and soil moisture memory in models depends on how well the physical processes are represented in the corresponding land surface model (Koster et al. 2002). As noted by Mitchell et al. (2004), significant disparities still exist between state-of-the-art land surface models that are forced over multiple annual cycles with identical surface forcing, including precipitation, because they differ in the parameterization of physical processes that account for the surface water and energy cycles. NARR is subject to the same constraints, and thus the results presented here carry an unavoidable amount of model dependence. The imbalances of the surface water budget remain under  $0.2 \text{ mm day}^{-1}$  on the time mean and less than  $0.5 \text{ mm day}^{-1}$  on individual months, with the exception of the basins in the mountainous west where the magnitude of the imbalances doubles. At least partially, the larger imbalances in the west result from not having included the snowpack analysis increments that result from the daily ingest of an external snow-cover analysis. Despite the lack of this correction term, the closeness to balance is superior to previous estimates from global reanalysis.

The diagnostics are performed within the framework of water or energy availability to sustain soil moisture anomalies. Evapotranspiration is not far from the potential evaporation in wet basins like the Columbia and Ohio basins, where the available water for evaporation exceeds the energy available for evaporation. Owing to

this and the dense summer-season vegetation cover over these wetter basins that can draw on deeper root-zone soil moisture, changes in near-surface shallow soil moisture have weaker correspondence to atmospheric variability in such basins (Table 3). In dry basins like the Colorado basin, the evapotranspiration is significantly smaller than the potential evaporation (available energy exceeds available water), and in this case the soil moisture anomalies are dissipated rapidly.

The summer relations between land surface and near-surface atmospheric variables were examined for North American basins with a wide diversity of climate regimes, from warm and dry to wet and cold. In general, dry and warm basins tend to have less cloud coverage, which in turn is associated with larger net short wave radiation and larger net longwave radiation, which tend to cancel each other. Hence the correspondingly more modest changes in total net radiation may increase or decrease with increasing basin dryness depending on the particular basin considered. Although the net total radiation does not have a clear relation to soil moisture, other energy terms do. This is the case of the evaporative fraction that depends on the surface sensible and latent heat fluxes: increases of soil moisture are related to increased evaporative fraction, more atmospheric humidity content, and consequently a lower LCL and increased cloud coverage.

As stated, weaker relations between soil moisture and all the other variables considered are found over the wetter basins, like the Ohio and Columbia basins, where no meaningful degree of precipitation–soil moisture correlation is found. However, the strength of the links as well as the lag correlation between soil moisture and precipitation increase in drier basins, like the core monsoon. We hypothesized that a region with low correlation between soil moisture and precipitation in NARR would not be expected to develop strong feedbacks of either sign between soil moisture and precipitation in nature. In other words, a high correlation of soil moisture and precipitation is a necessary but not sufficient condition for a feedback to exist between them. These regions of higher correlations may sustain land–atmosphere feedbacks that contribute to the predictive skill of precipitation. The results reinforce the concept that predictive skill could be improved over certain regions (particularly those not too wet) with an adequate representation of the surface conditions. The choice of monthly data may impose limits to the new understanding and insight of the soil moisture–precipitation interactions to be gained from this study. We plan to investigate the dependence of such interactions on time scales from days to seasons, and for deeper soil moisture regimes, as they could exhibit a better corre-

spondence responding to physical scales rather than the arguably arbitrary 1-month scale.

*Acknowledgments.* The careful reviews and useful comments of three anonymous reviewers are much appreciated. The authors also thank Dr. E. Kalnay, Dr. F. Mesinger, and the NCEP team that developed the NARR, as they provided useful input at different stages of the study. This research was supported by NOAA Grants NA17EC1483 and NA04OAR4310164.

Alan Betts acknowledges support from NSF under Grant ATM-0529797, and from NASA under Grant NNG05GQ88A.

#### REFERENCES

- Beljaars, A. C. M., P. Viterbo, M. J. Miller, and A. K. Betts, 1996: The anomalous rainfall over the United States during July 1993: Sensitivity to land surface parameterization and soil moisture anomalies. *Mon. Wea. Rev.*, **124**, 362–383.
- Berbery, E. H., 2001: Mesoscale moisture analysis of the North American monsoon. *J. Climate*, **14**, 121–137.
- , Y. Luo, K. E. Mitchell, and A. K. Betts, 2003: Eta model estimated land surface processes and the hydrologic cycle of the Mississippi basin. *J. Geophys. Res.*, **108**, 8852, doi:10.1029/2002JD003192.
- Betts, A. K., 2007: Coupling of water vapor convergence, clouds, precipitation, and land-surface processes. *J. Geophys. Res.*, **112**, D10108, doi:10.1029/2006JD008191.
- , and J. H. Ball, 1998: FIFE surface climate and site-average dataset 1987–89. *J. Atmos. Sci.*, **55**, 1091–1108.
- , and P. Viterbo, 2005: Land-surface, boundary layer, and cloud-field coupling over the southwestern Amazon in ERA-40. *J. Geophys. Res.*, **110**, D14108, doi:10.1029/2004JD005702.
- , J. H. Ball, A. C. M. Beljaars, M. J. Miller, and P. A. Viterbo, 1996: The land surface-atmosphere interaction: A review based on observational and global modeling perspectives. *J. Geophys. Res.*, **101**, 7209–7225.
- , P. Viterbo, A. Beljaars, H.-L. Pan, S.-H. Hong, M. Goulden, and S. Wofsy, 1998: Evaluation of land-surface interaction in the ECMWF and NCEP/NCAR reanalysis models over grassland (FIFE) and Boreal forest (BOREAS). *J. Geophys. Res.*, **103**, 23 079–23 085.
- Bosilovich, M. G., and W.-Y. Sun, 1999: Numerical simulation of the 1993 midwestern flood: Land–atmosphere interactions. *J. Climate*, **12**, 1490–1505.
- Chen, F., and Coauthors, 1996: Modeling of land surface evaporation by four schemes and comparison with FIFE observations. *J. Geophys. Res.*, **101**, 7251–7268.
- , Z. Janjić, and K. Mitchell, 1997: Impact of atmospheric surface-layer parameterizations in the new land-surface scheme of the NCEP mesoscale Eta model. *Bound.-Layer Meteor.*, **85**, 391–421.
- Daly, C., R. P. Neilson, and D. L. Phillips, 1994: A statistical-topographic model for mapping climatological precipitation over mountainous terrain. *J. Appl. Meteor.*, **33**, 140–158.
- Delworth, T., and S. Manabe, 1988: The influence of potential evaporation on the variabilities of simulated soil wetness and climate. *J. Climate*, **1**, 523–547.
- , and —, 1989: The influence of soil wetness on near-surface atmospheric variability. *J. Climate*, **2**, 1447–1462.
- Dirmeyer, P. A., 2003: The role of land surface background state in climate predictability. *J. Hydrometeor.*, **4**, 599–610.
- Ek, M. B., K. E. Mitchell, Y. Lin, E. Rogers, P. Grunmann, V. Koren, G. Gayno, and J. D. Tarpley, 2003: Implementation of Noah land surface model advances in the National Centers for Environmental Prediction operational mesoscale Eta model. *J. Geophys. Res.*, **108**, 8851, doi:10.1029/2002JD003296.
- Eltahir, E. A. B., 1998: A soil moisture-rainfall feedback mechanism. 1. Theory and observations. *Water Resour. Res.*, **34**, 765–776.
- Entekhabi, D., 1995: Recent advances in land-atmosphere interaction research. *Rev. Geophys.*, **33**, 995–1003.
- , I. Rodriguez-Iturbe, and R. L. Bras, 1992: Variability in large-scale water balance with land surface-atmosphere interaction. *J. Climate*, **5**, 798–813.
- Findell, K. L., and E. A. B. Eltahir, 2003: Atmospheric controls on soil moisture–boundary layer interactions. Part I: Framework development. *J. Hydrometeor.*, **4**, 552–569.
- Gochis, D. J., W. J. Shuttleworth, and Z.-L. Yang, 2003: Hydro-meteorological response of the modeled North American monsoon to convective parameterization. *J. Hydrometeor.*, **4**, 235–250.
- Gutzler, D. S., 2000: Covariability of spring snowpack and summer rainfall across the southwest United States. *J. Climate*, **13**, 4018–4027.
- Hong, S.-Y., and E. Kalnay, 2000: Origin and maintenance of the Oklahoma–Texas drought of 1998. *Nature*, **408**, 842–845.
- , and —, 2002: The 1998 Oklahoma–Texas drought: Mechanistic experiments with NCEP global and regional models. *J. Climate*, **15**, 945–963.
- Koren, V., J. Schaake, K. Mitchell, Q. Duan, F. Chen, and J. Baker, 1999: A parameterization of snowpack and frozen ground intended for NCEP weather and climate models. *J. Geophys. Res.*, **104**, 19 569–19 585.
- Koster, R. D., and M. J. Suarez, 2003: Impact of land surface initialization on seasonal precipitation prediction and temperature prediction. *J. Hydrometeor.*, **4**, 408–423.
- , —, and M. Heiser, 2000: Variance and predictability of precipitation at seasonal-to-interannual timescales. *J. Hydrometeor.*, **1**, 26–46.
- , P. A. Dirmeyer, A. N. Hahmann, R. Ijpelaar, L. Tyahla, P. Cox, and M. J. Suarez, 2002: Comparing the degree of land–atmosphere interaction in four atmospheric general circulation models. *J. Hydrometeor.*, **3**, 363–375.
- , and Coauthors, 2004: Regions of strong coupling between soil moisture and precipitation. *Science*, **305**, 1138–1140.
- Lin, Y., K. E. Mitchell, E. Rogers, M. E. Baldwin, and G. J. DiMego, 1999: Test assimilations of the real-time, multi-sensor hourly precipitation analysis into the NCEP Eta model. Preprints, *Eighth Conf. on Mesoscale Meteorology*, Boulder, CO, Amer. Meteor. Soc., 341–344.
- Liu, Y., and R. Avissar, 1999: A study of persistence in the land–atmosphere system using a general circulation model and observations. *J. Climate*, **12**, 2139–2153.
- Luo, Y., E. H. Berbery, and K. E. Mitchell, 2005: The operational Eta model precipitation and surface hydrologic cycle of the Columbia and Colorado basins. *J. Hydrometeor.*, **6**, 341–370.
- Mahrt, L., and M. Ek, 1984: The influence of atmospheric stability on potential evaporation. *J. Climate Appl. Meteor.*, **23**, 222–234.
- , and H. Pan, 1984: A two-layer model of soil hydrology. *Bound.-Layer Meteor.*, **29**, 1–20.

- Mesinger, F., and Coauthors, 2006: North American Regional Reanalysis. *Bull. Amer. Meteor. Soc.*, **87**, 343–360.
- Mitchell, K. E., and Coauthors, 2004: The multi-institution North American Land Data Assimilation System (NLDAS): Utilizing multiple GCIP products and partners in a continental distributed hydrological modeling system. *J. Geophys. Res.*, **109**, D07S90, doi:10.1029/2003JD003823.
- Namias, J., 1958: Persistence of mid-tropospheric circulations between adjacent months and seasons. *The Atmosphere and Sea in Motion; Scientific Contributions to the Rossby Memorial Volume*, B. Bolin, Ed., Rockefeller Institute Press, 240–248.
- Paegle, J., K. C. Mo, and J. Nogués-Paegle, 1996: Dependence of simulated precipitation on surface evaporation during the 1993 United States summer floods. *Mon. Wea. Rev.*, **124**, 345–361.
- Pan, H.-L., and L. Mahrt, 1987: Interaction between soil hydrology and boundary-layer development. *Bound.-Layer Meteor.*, **38**, 185–202.
- Roads, J., and A. Betts, 2000: NCEP–NCAR and ECMWF reanalysis surface water and energy budgets for the Mississippi River basin. *J. Hydrometeor.*, **1**, 88–94.
- , and Coauthors, 2003: GCIP water and energy budget synthesis (WEBS). *J. Geophys. Res.*, **108**, 8609, doi:10.1029/2002JD002583.
- Robock, A., and Coauthors, 2003: Evaluation of the North American Land Data Assimilation System over the southern Great Plains during the warm season. *J. Geophys. Res.*, **108**, 8846, doi:10.1029/2002JD003245.
- Schaake, J. C., V. I. Koren, Q.-Y. Duan, K. Mitchell, and F. Chen, 1996: Simple water balance model for estimating runoff at different spatial and temporal scales. *J. Geophys. Res.*, **101**, 7461–7476.
- Schlosser, C. A., and P. C. D. Milly, 2002: A model-based investigation of soil moisture predictability and associated climate predictability. *J. Hydrometeor.*, **3**, 483–501.
- Shukla, J., and Coauthors, 2000: Dynamical seasonal prediction. *Bull. Amer. Meteor. Soc.*, **81**, 2593–2606.
- Small, E. E., 2001: The influence of soil moisture anomalies on variability of the North American monsoon system. *Geophys. Res. Lett.*, **28**, 139–142.
- Stephens, G. L., 2005: Cloud feedbacks in the climate system: A critical review. *J. Climate*, **18**, 237–273.
- Trenberth, K. E., and C. J. Guillemot, 1996: Physical processes involved in the 1988 drought and 1993 floods in North America. *J. Climate*, **9**, 1288–1298.
- Xie, P., and P. A. Arkin, 1997: Global precipitation: A 17-year monthly analysis based on gauge observations, satellite estimates, and numerical model outputs. *Bull. Amer. Meteor. Soc.*, **78**, 2539–2558.